3D VISCO-ELASTIC WAVE PROPAGATION IN THE BORREGO VALLEY, CALIFORNIA

Kim B OLSEN[1], Robert L NIGBOR[2] And Takaaki KONNO[3]

SUMMARY

We have simulated 2-Hz wave propagation in a three-dimensional model of the Borrego Valley, southern California, for a **M** 4.9 earthquake with epicenter 5 km north of the valley. A fourth-order staggered-grid finite-difference method was used to calculate viscoelastic ground motion in a basin model (9 km by 5 km by 0.4 km) consisting of heterogeneous sediments surrounded by bedrock. We simulated the earthquake as a double-couple point source and computed the ground motions in the valley separately for the parts of the source incident from below and from the North. The earthquake was recorded by a surface array as well as a deep downhole array (0 - 238 m depth) in the center of the valley, all equipped with digital three-component seismic instruments. The simulation reproduces the overall pattern of ground motions at basin and borehole sites and shows a good correlation of observed to synthetic waveforms. In particular, the 3D simulation reproduces the recorded peak motions, cumulative kinetic energies, and Fourier spectral amplitudes within a factor of 2 for most components at the individual sites. The correlation between data and simulation allows us to identify the secondary arrivals in the records as Love and Rayleigh waves generated at the edges of the valley and the troughs of the basin. The peak velocities for the waves incident onto the valley from below are generally more than an order of magnitude larger than those for the waves incident from the North. The success of the prediction requires the inclusion of anelastic attenuation in the simulation with Q values for P- and S-waves in the saturated alluvium (S-wave velocity of 300 m/s) of about 30. We also used a profile of the 3D model and the soil parameters at the deep borehole to examine the ability of 2.5D and 1D model approximations to predict the data. The maximum peak velocities and total cumulative kinetic energies are reproduced at the recording sites within a factor of 2 for both 2.5D and 1D model approximations, but are underpredicted by up to an order of magnitude at some depths for individual components. In particular, the 2.5D and 1D simulations tend to underpredict the duration.

INTRODUCTION

The recent appearance of more powerful computers, better constrained basin models, and more efficient numerical wave propagation codes, have facilitated computation of the 3D low-frequency seismic response of sedimentary basins (e.g., Frankel and Vidale, 1992; Yomogida and Etgen, 1993; Olsen et al., 1995; Olsen and Archuleta, 1996). Due to large computational requirements, the 3D simulations have generally been limited to unrealistically large minimum velocities (0.5-1 km/s), and the bandwidth has generally been limited to frequencies less than 1 Hz. However, these studies demonstrated significant 3-D effects from the basin structures, including a strong sensitivity of the shaking duration to the location in the basin, and the generation of surface waves at the edges of the basin.

The Borrego Valley seismic observatory represents an excellent site for testing the accuracy of state-of-the-art 3D wave propagation techniques, with direct borehole constraints on the incoming wavefield. The Upper Borrego Valley is limited in size to about 9 km by 5 km and is equipped with surface and downhole high-

resolution three-component, digital seismic instrumentation and the seismic velocities and densities of the underlying basin sediments have been accurately mapped by a variety of geophysical methods. The deepest borehole instrument is located 238 m below the valley's surface in the bedrock underlying the basin sediments.

While significant 3D ground motion amplification effects are reported for sedimentary basins throughout the world, an important question in ground motion modeling is to what extent the geometry of a specific sedimentary basin affects the ground motion. If it can be shown that the ground motion amplification due to the 3D basin structure is insignificant, or if 2.5D or even 1D approximations of the earth model appear sufficient to accurately model wave propagation, tremendous computer resources can be saved in future estimations of ground motion. For this reason, we compare seismograms for 1D, 2.5D, and 3D simulations of a **M** 4.9 scenario earthquake to both surface and borehole recordings in the Borrego Valley.

BORREGO VALLEY MODEL AND SEISMIC INSTRUMENTATION

The Borrego Valley is located in the desert of southern California in an area of relatively high seismicity, consisting mostly of right-lateral strike-slip events from north-west/south-east trending faults. For this reason, and due to the limited size of the valley and thickness of the underlying sediments (less than 400 m), the Borrego Valley was deployed with both a surface and downhole array of high-resolution three-component digital seismic instrumentation (Figure 1).
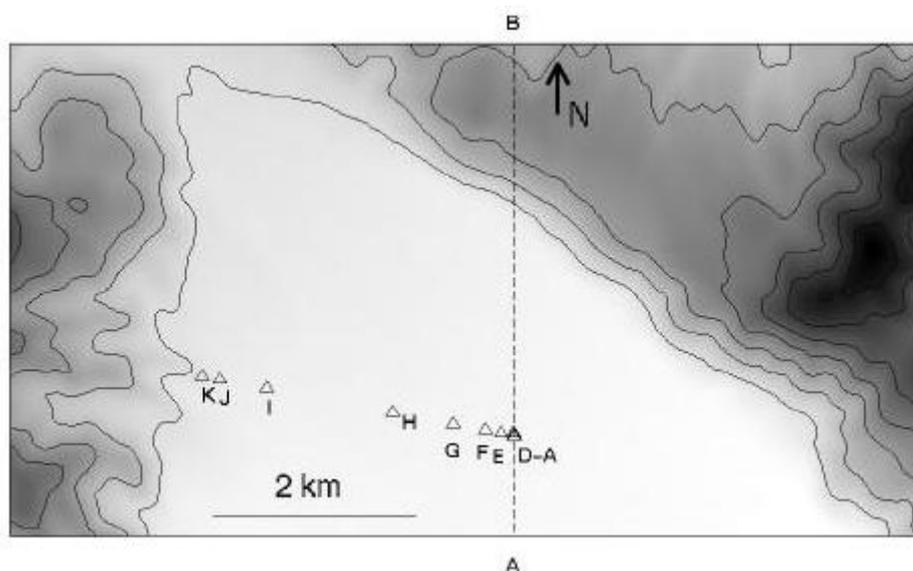

Figure 1. Upper Borrego Valley model and seismic instrumentation. The contours depict surface topography with a contour interval of 100 m. The triangles denote the location of surface recording sites. The deep borehole is located at station A. Profile A-B is used for 2.5D modeling.

The 3D model of the Upper Borrego Valley consists of sediments surrounded by bedrock. The seismic velocities of the sediments and bedrock as well as the sediment/bedrock boundary were estimated by 3D inversion of gravity data and interpretation of seismic reflection and refraction lines and borehole logs from the downhole array. Based on the surveys the sediments are separated into unsaturated and saturated alluvium. P- and S-wave velocities and densities for the unsaturated alluvium vary between 0.5-1.2 km/s, 0.3-0.65 km/s, and 1.9-2.1 g/cm3, respectively. P- and S-wave velocities and densities for the saturated alluvium vary between 1.9-2.3 km/s, 0.65-0.8 km/s, and 2.2-2.3 g/cm3, respectively. The borehole was deployed with instruments at depths of 0 m, 9.4 m, 19.4 m, 138 m, and 238 m below the valley surface. The deepest instrument is located in bedrock, about 10 m below the lower boundary of the sediments. P- and S-wave velocities and densities for bedrock are 5.2 km/s, 3.0 km/s, and 2.65 g/cm3, respectively.

With frequencies up to 2 Hz and a minimum shear wave velocity as low as 0.3 km/s we expect significant effects from attenuation in the Borrego Valley. Unfortunately, Q is the elastic parameter with the largest uncertainty in the Borrego Valley model. We used trial-and-error modeling to estimate the distributions of Qs and Qp that generate synthetics with an optimal fit to data, in particular for the amplitude of the reverberations following the

initial arrival where anelastic attenuation is most effective. We find that values of both Qs and Qp of 30 in the sediments, and Qs=0.1Vs (m/s) in rock gives the best fit between synthetics and data.

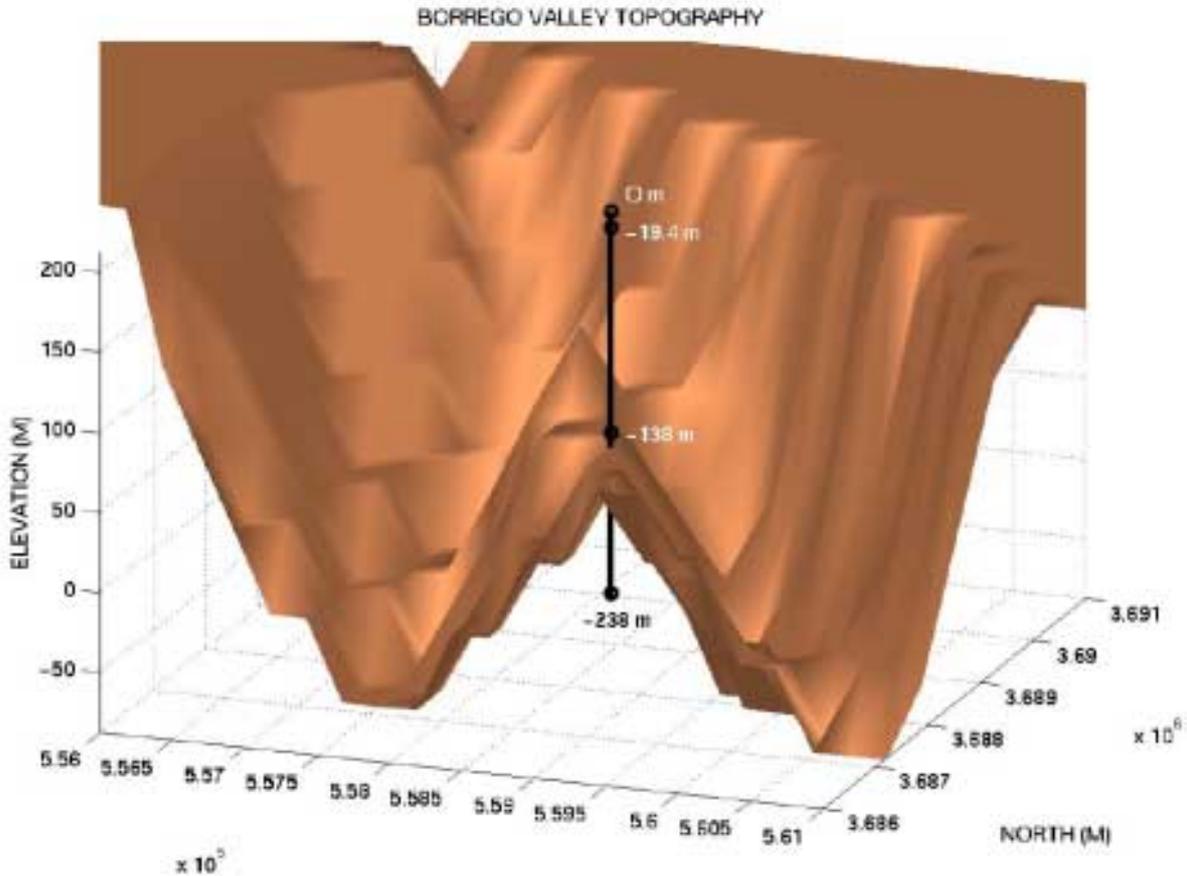**Figure 2. 3D perspective of the isosurface for Vs = 1 km/s, superimposed with the borehole array. Note that the borehole array is located on a ridge in between two deeper troughs of the basin.**

The equipment at each station consists of Kinemetrics FBA-23 accelerometers (ALTUS series with 20-bit digital recording). We included data from the surface array for 11 stations, of which 10 (A-J) are located on unconsolidated sediments in the Borrego Valley and one (K) is located on a bedrock outcrop in the mountains to the west of the valley (Figure 1). Borehole data is used at depths of 9.4 m, 19.4 m, 138 m, and 238 m at the main station in the center of the valley.

FINITE-DIFFERENCE MODELING AND EARTHQUAKE SCENARIO

We use a fourth-order staggered-grid finite-difference scheme to solve the 3D viscoelastic equations of motion (Robertsson et al., 1994). Viscoelasticity is implemented using stress relaxation independently for P and S waves. We use the absorbing boundary conditions by Clayton and Engquist (1977), and the sides of the computational model are padded with homogeneous regions of attenuative material to furthermore limit reflections from the boundaries of the grid (Cerjan et al., 1985).

Our scenario earthquake is selected as the **M** 4.9 earthquake that occurred on 26 July 1997 with epicenter about 5 km north of the valley and a hypocentral depth of 12.7 km. The earthquake was recorded by 11 surface stations and a deep and 2 shallow borehole arrays in the valley. We used at right-lateral strike-slip focal mechanism on a vertical fault with a strike of 306°, in general agreement with estimates from the U.S. Geological Survey and the Southern California Earthquake Center, and with the general trend of the Coyote Creek and San Jacinto faults.

We simulated the **M** 4.9 earthquake in a two-step proceduere, in a fashion similar to that obtained by a variable-grid finite-difference implementation. However, in order to demonstrate the relative contribution of energy impinging onto the Upper Borrego Valley from below and from the North for the earthquake, we carried out two different sets of simulations. First, a double-couple point source with a rise time of 0.35 sec was inserted at the hypocenter location given by the U.S. Geological Survey. The point source was simulated in two different models with a grid spacing of 100 m and P- and S-wave velocities and densities defined by the regional model by Hadley and Kanamori (1977), (1) one with absorbing boundary conditions and (2) one with a free surface at the top of the model. The stress tensor for the wavefield was saved at a sheet of node points located at a datum plane 400 m below the surface for simulation (1), just below the deepest sediments of the Borrego Valley model, and along a vertical sheet extending from the surface to a depth of 400 m for simulation (2). Secondly, the stress-time histories for the simulations (1) and (2) described above are imposed in models using a grid spacing of 25 m and including the 3-D Borrego Valley velocity model. Using a modeling resolution of 5 points per wavelength, this discretization enables us to simulate wave propagation up to 2 Hz in a model where near-surface shear wavelengths are on the order of 150 m. The Borrego Valley model (approximately 9 km by 5 km by 1.25km) is discretized into 3.7 million grid points.

PEAK VELOCITIES

The peak velocities in the Borrego Valley are shown in Figure 3, superimposed with depth contours for the isosurface of Vs=1 km/s. The north-south component contains the strongest effects of the source and represents the largest peak velocities. Note the significant basin edge effects, in particular along the eastern boundary of the valley. Some of the largest amplitudes are found along the relatively steeply-dipping eastern edge of the valley. This is in agreement with results from other 3D scenario modeling studies (e.g., Olsen et al., 1995; Olsen and Archuleta, 1996), where some of the strongest ground motion amplification were found near the steepest-dipping basin edges. Another striking pattern in the peak velocities is the increased amplification immediately behind convex-shaped parts of the basin edges or bottom (e.g., below the north-south trending trough below station H. Such amplification pattern was noticed for 3D simulations of wave propagation in the Weber Basin, Utah (Olsen and Schuster, 1994) and identified as focusing effects at the convex-shaped boundaries of the basin. The reason why the focusing occurs for the wavefield impinging from below the valley is that the convex-shaped parts of the sediment-bedrock interface at the edge of the valley tend to maintain their cylindrical structure from the surface to a limited depth, dipping towards the center of the valley.

COMPARISON OF SIMULATED AND OBSERVED SEISMOGRAMS

Figure 4 compares observed 0.1-2 Hz velocity seismograms for the **M** 4.9 earthquake at surface stations to the synthetics. The observed traces are aligned with the simulated ones using the arrival with the largest amplitude, at about 3 sec on the north-south component. The observed seismograms show a good agreement in the maximum amplitudes, duration, and general waveforms of significant wave trains at most sites. Due to the relatively small distances between stations A-F (see Figure 1), the waveforms recorded at these sites are fairly similar. As expected, the best correlation of waveforms for the synthetics and data is obtained for the initial arrivals, which are predominantly controlled by the source, but also for later arriving phases. For example, the synthetics reproduce a secondary arrival 2-3 sec after the initial S wave at stations A-F and H, particularly clear on the horizontal components. Snapshots of the wave propagation show that this phase is a Love wave generated by conversion at the eastern slope of the eastern-most trough of the basin. This phase is followed by a Rayleigh wave generated at the eastern edge of the valley (arriving at about 14 s at the main station). The large-amplitude phase on the north-south component arriving at the main station at about 10 s, also reproduced by the simulation, is identified as a Love wave generated at the western edge and nearby trough of the basin. At station H, located above the deepest part of the western trough of the basin, the energy immediately following the initial arrival is likely generated by mostly vertical resonance effects. At station I, the relatively large-amplitude phase arriving at 3.5-4.5 s is a Love generated at the western edge of the basin. This phase is amplified by superposition of it's weaker counterpart from the eastern edge of the basin to generate the relatively large-amplitude phase arriving at 7-8 s at station H. While the general agreement between synthetics and data is good, however, at some sites, particularly on the east-west and vertical components, the synthetics tend to underpredict the recorded durations somewhat. This discrepancy suggests a lack of complexity in the basin model. The variation of peak velocities generally agrees for synthetics and data across the surface array. The peak velocities for stations A-G in the center of the valley are characterised by relatively large values on the north-south component above the bedrock

high shown in Figure 2. At station H, the peak velocity increases in the simulation due to influence of the western trough of the basin (see Figure 2), in agreement with data. At station I, the peak velocity has decreased for both data and synthetics above the shallowing sediments towards the west. The basin-edge effect has increased the peak velocities on the synthetics at the shallow alluvium site J to values larger than those for the data, in particular for the east-west and vertical components, while peak velocities for data and synthetics at the rock site K are in much closer agreement. The discrepancy at station J is likely related to uncertainty of the shape of the nearby basin edge. The energy arriving from below is much stronger than that incident from North, as expected from the near-vertical incidence angle of the earthquake. For this reason, the synthetics for the wavefield impinging from below is very similar to the combined synthetics, shown in Figure 4.
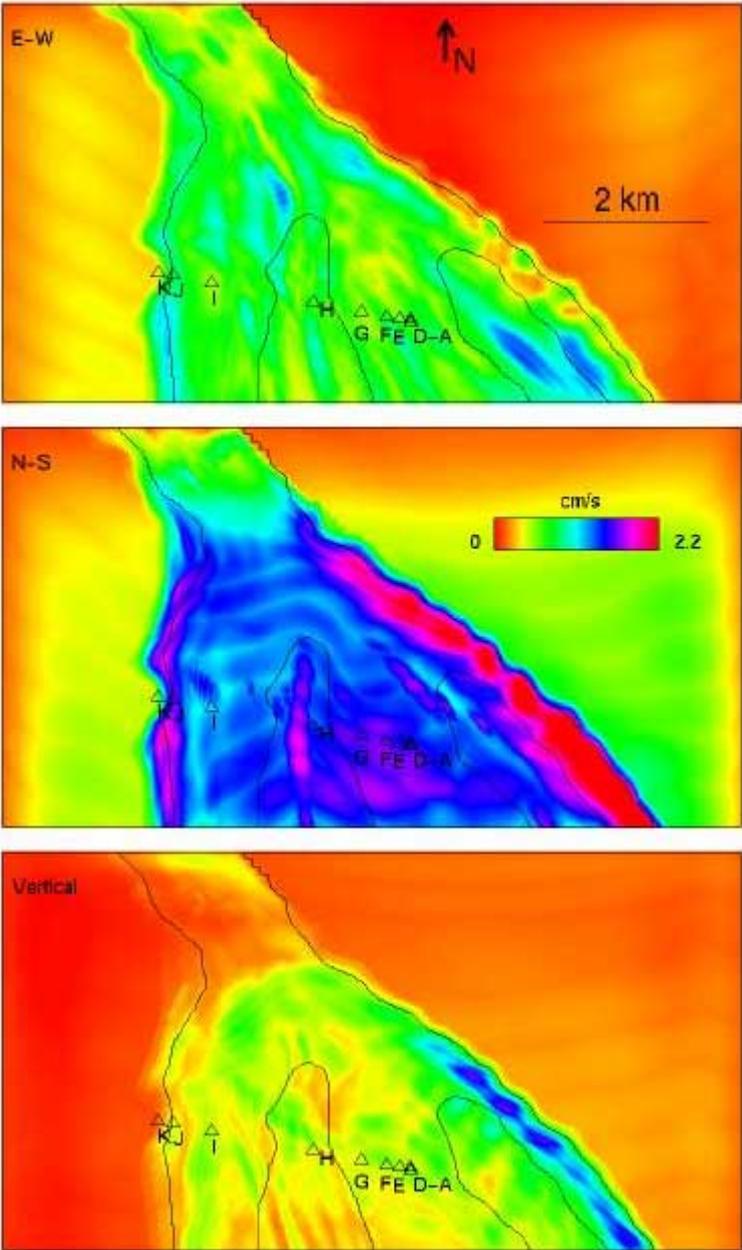

Figure 3. Maps of peak velocities in the Borrego Valley for a simulation of the M 4.9 earthquake, superimposed with the depth contours of 0.1 km and 0.3 km for the isosurface of Vs=1 km/s. The triangles depict the location of the borehole array and the rock station. The peak velocities are scaled by the same constant for all components.
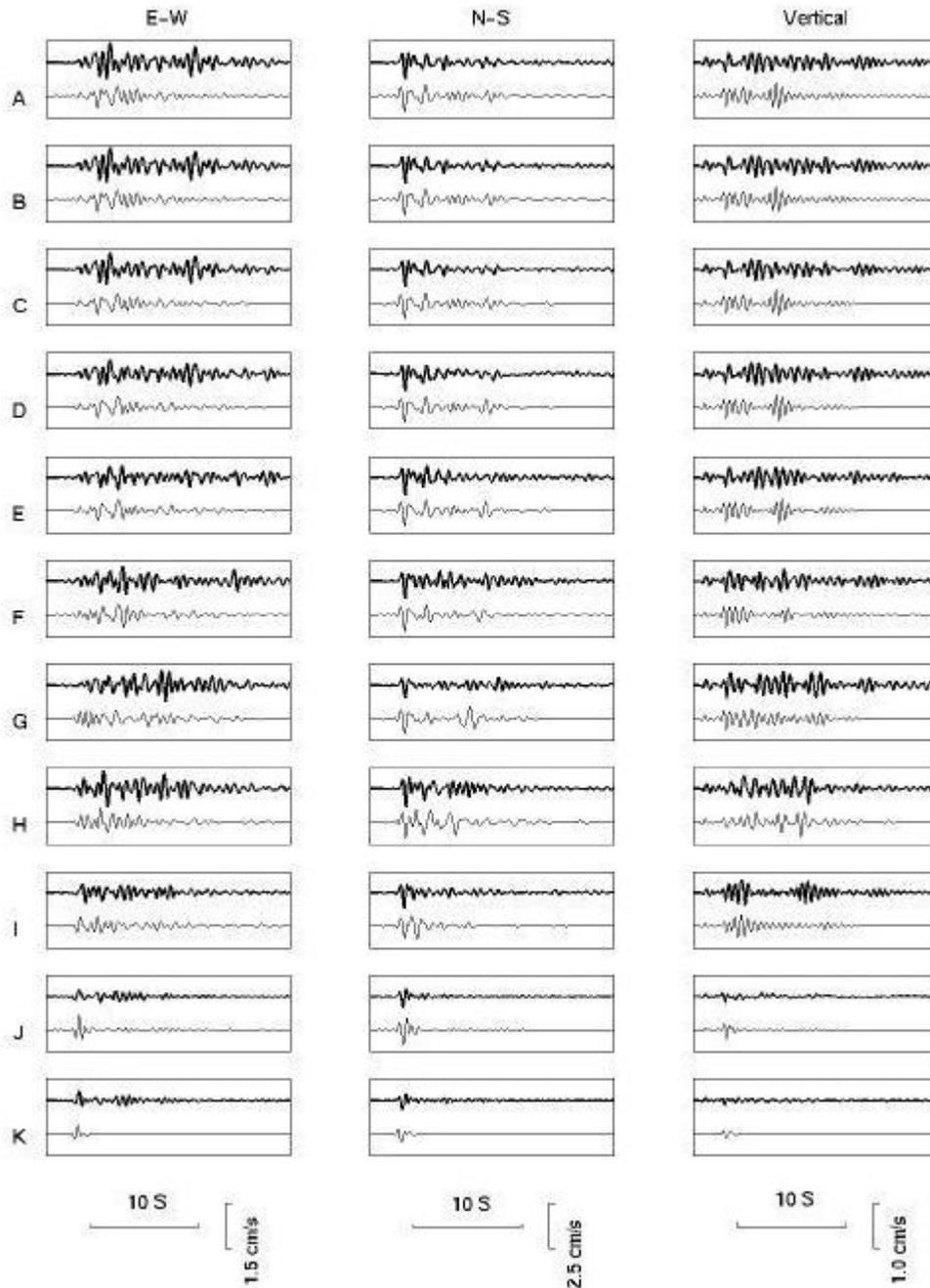
Figure 4. Comparison of simulated velocity seismograms for the M 4.9 earthquake to data (thick traces) at 11 surface recording sites (A-K, see Figure 1).

1D AND 2.5D AMPLIFICATION EFFECTS

Figure 5 compares velocity seismograms for 3D, 2.5D and 1D simulations with the **M** 4.9 earthquake for the borehole array at the main station. The model for the 2.5D simulation is a vertical cross section of the 3D Borrego Valley model taken along profile A-B shown in Figure 1. This profile intersects the estimated hypocenter of the earthquake and the main station with the borehole array within 0.5 km. The waves are propagated using the fourth-order 3D finite-difference method, where the 2-D cross section was extended in the east-west direction. The 1D model is the layered representation of the 3D Borrego Valley model at the main station. Note the strong similarity between the 1D, 2.5D and 3D responses on the vertical component and the horizontal component with largest amplitude (north-south) for the initial P and S arrivals. The synthetics reproduce the increase in amplitude for the data up through the sediments, reflecting the change in impedance

and show good fits of waveform for data and synthetics, in particular for the first 5 seconds. The negligible variation in timing of the secondary arrivals with depth supports that they are surface waves. As observed for
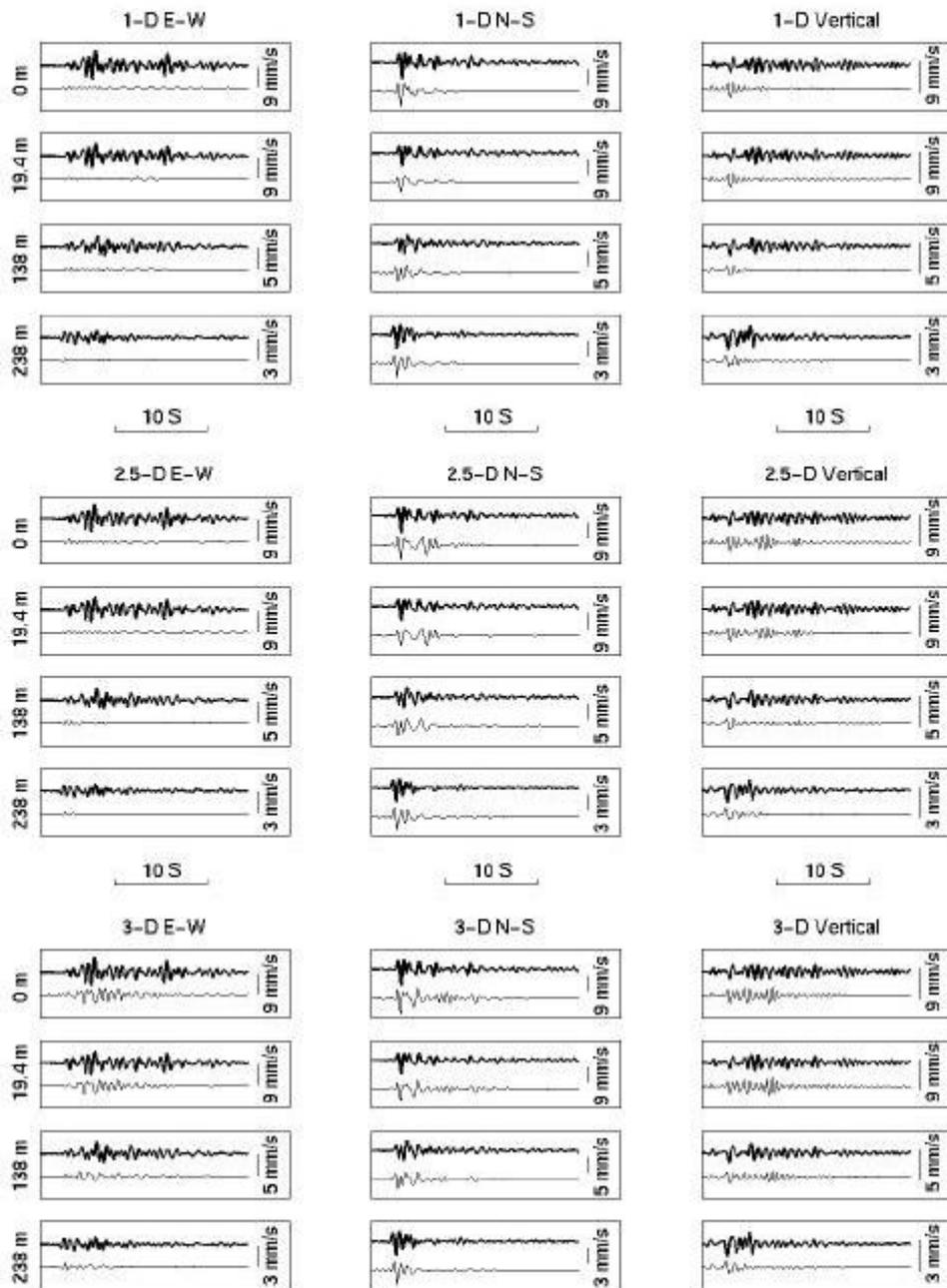

Figure 5. Comparison of 3D, 2.5D, and 1D synthetics with data (thick traces) at the deep borehole array.

some of the surface stations, the synthetics underpredict the durations somewhat for some components. While absent in the 1D synthetics, the 2.5D and 3D simulations reproduce the secondary phase 2-3 seconds after the initial S wave on the north-south component, as noticed in the 3D synthetics for the surface array (Figure 4). However, the 2.5D and in particular the -D synthetics tend to underpredict the duration on all components, due to insufficient amounts of mode conversion and surface wave generation, and both 1D and 2.5D simulations fail almost completely to generate any of the significant phases on the east-west component.

CONCLUSIONS

Our simulation of 2-Hz viscoelastic wave propagation in a complex 3D model of the Borrego Valley reproduces the overall waveforms, peak velocities, cumulative kinetic energies and Fourier spectra at surface and borehole sites from a nearby **M** 4.9 earthquake within a factor of 2 for most components. The best fit of the synthetics to data is obtained for Q values for P and S waves in the sediments of about 30. Due to the correlation between data and simulation, we are able to identify secondary arrivals in the data as Rayleigh and Love waves generated at the edges and troughs of the basin. The largest peak velocities are associated with the north-south component, dominated by the source, along the edges and above some of the deepest parts of the basin, due to focusing and surface wave generation. By far, most of the energy enters the valley from below. In fact, this part of the wavefield is an order of magnitude larger than that impinging onto the valley from the North. We used a profile of the 3D model and the soil parameters at the borehole to examine the ability of 2.5D or 1D model approximations to predict the data. Both 2.5D and 1D model approximations underpredict the peak velocities on some individual components by up to an order of magnitude. Our results suggest that 3D effects from the basin structure, the near-surface low-velocity layer, and attenuation on seismic wave propagation all significantly influence site amplification in the Borrego Valley. Future modeling of site amplification in the Borrego Valley should include all of these phenomena.

REFERENCES

Cerjan, C., D. Kosloff, R. Kosloff, and M. Reshef (1985). "A nonreflecting boundary condition for discrete acoustic and elastic wave equations", *Geophysics* 50, 705-708.

Clayton, R., and B. Engquist (1977). "Absorbing boundary conditions for acoustic and elastic wave equations", *Bull. Seism. Soc. Am.* 71, 1529-1540.

Frankel, A., and J. Vidale (1992). "A three-dimensional simulation of seismic waves in the Santa Clara Valley, California, from a Loma Prieta aftershock", *Bull. Seism. Soc. Am.* 82, 2045-2074.

Hadley, D. and H. Kanamori (1977). "Seismic structure of the Transverse Ranges, California", *Geol. Soc. Am. Bull.* 88, 1469-1478.

Olsen, K.B. (1994). "Simulation of three-dimensional wave propagation in the Salt Lake Basin", *Ph.D. Thesis*, University of Utah.

Olsen, K.B., and G.T. Schuster (1994). "Three-dimensional Modeling of Site Amplification in East Great Salt Lake Basin", *USGS Technical Report* 1434-93-G-2345.

Olsen, K.B., R.J. Archuleta, and J.R. Matarese (1995). "Three-dimensional simulation of a magnitude 7.75 earthquake on the San Andreas fault", *Science* 270, 1628-1632.

Olsen, K.B. and R.J. Archuleta (1996). "Three-dimensional simulation of earthquakes on the Los Angeles fault system", *Bull. Seism. Soc. Am.* 86 575-596.

Robertsson, J.O.A., J.O. Blanch, and W.W. Symes (1994). "Viscoelastic finite-difference modeling", *Geophysics* 59, 1444-1456.